

THE INFLUENCE OF INDUCTION HARDENING PROCESS PARAMETERS ON THE PROPERTIES OF 50CrMo4 STEEL

C. GABOR¹ D. CRISTEA¹ D. MUNTEANU¹ T. BEDO¹
M.A. POP¹ S.I. MUNTEANU¹ I. MILOŞAN¹

Abstract: *Induction hardening can be used to improve the surface properties of large bearing rings, with the advantage that heating the part in its entirety is not required. However, several problems can occur: uneven depth of the hardened layer in different zones along the ring circumference, uneven depth of the hardened layer reported in the ring section, and cracks in the bearing material. Therefore, the optimization of the induction process is desired. The specific parameters involved in the quenching operation and their influence on the surface hardening depth were observed.*

Key words: *induction hardening, surface hardening depth, hardness.*

1. Introduction

Hardening is a process used to increase the hardness of a steel part. The first step for hardening is heating the components in the austenite domain. The material is then quenched by cooling the material, with various cooling rates, depending on the desired final structure. In the case of surface hardening, high cooling rates should be achieved so that most of the austenite phase is transformed to martensite by a diffusionless phase transition, producing the desired hardening effect [7].

Compared to the established heating methods, induction hardening has important advantages, such as: fast heating rate, good reproducibility and low energy consumption [2]. Another advantage of induction hardening is that it can be applied only on specific regions (surface layer, pins, gear teeth), leaving the properties of the remaining zones unchanged. During induction heating an alternating current is flowing through a copper coil. This generates a rapidly changing magnetic field. The work-piece is placed within the magnetic field, which invokes eddy currents in the conductive section. These currents heat the material until the desired temperature is reached. The cooling stage follows, using various quenching mediums, which leads to the desired phase transformation.

Effective induction heating relies on the proper design and manufacture of the inductive coils. Heating rates and uniformity performance may vary among inductive coil designs. Real-life induction hardening experiments are often very expensive and difficult to implement. Mathematical analysis and numerical simulations could contribute significantly to the design process, with significantly diminished costs [1].

¹ Materials Science and Engineering Faculty, *Transilvania* University of Braşov.

Although inductive hardening is widely used, the needs for process optimization are still open. Therefore, several authors studied the processes of induction heating and reported mathematical model simulation results [3-6], [8-11]. One of the most popular alloy steels used in the industry and also studied by other authors is 42CrMo4 [1]. However, other grades of steel might behave differently during induction quenching, thus the need for further studies.

2. Experimental Details

The steel grade studied is 50CrMo4 (AISI 4150, 1.7228) typically designated to a hardening process followed by a tempering process leading in the end to the sorbite structure. The chemical composition of this steel is: 0.46-0.54% C, 0.5-0.8% Mn, 0.9-1.2% Cr, 0.15-0.30% Mo, max. 0.035% S, max. 0.025% P, max. 0.4% Si. Molybdenum has a strong influence in reducing the brittleness and obtaining a fine grain structure.

Depending on their size, bearing rings are typically produced by deformation (forging, pressing or rolling) or by material removal (turning). Hardening followed tempering will be applied on the semi-finished bearing ring in order to overcome the dendritic casting structure and the reduction of the anisotropy of the material, as well as the even distribution of carbides (in alloyed steels).

The desired result is to obtain on the active surface of the bearing ring a hardened layer with uniform thickness on both the circumference of the ring and in section, with a predetermined thickness (SHD - surface hardening depth). The main advantages of this process are: a significantly shortened heat treatment, of about 2 h; the material used to produce the induction hardened rings is cheaper; the investment cost is significantly reduced, compared to the classic method.

The desired characteristics regarding the material properties are different for several zones of the bearing ring. These zones are presented in Figure 1, with their characteristics as follows: i) for zone A (rolling path and board) the desired hardness to be obtained after the induction hardening process is 60 ± 2 HRC, with a surface hardening depth of at least 5.9 mm. The hardness is measured at several control points: at a distance of 5 mm from the boards of the ring, on the rolling path; in the middle of the rolling path from the board of the ring; on the board of the ring; ii) for zone B, the goal in terms of hardness value is 53 HRC with a surface hardening depth of minimum 3.3 mm.

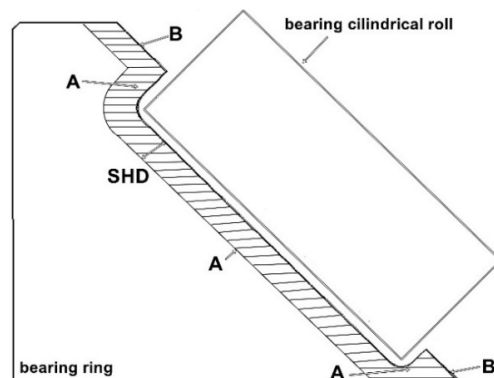


Fig. 1. *Bearing ring section:*
A - rolling path B - board; SHD - surface hardening depth

3. Results and Discussion

The samples analyzed in terms of the optimal induction hardening parameters were cut and prepared for hardness measurements and metallographic analysis with the help of Struers LaboTom cutting machine, and Struers LaboPol and Buehler Phoenix Beta polishing machines. The hardness was measured with the Future-Tech FM700 micro-hardness tester. The medium hardness values measured on the samples are as follows: 28.26 HRC before the hardening process, 33.38 HRC in the intermediary/interface area between the hardened zone and the raw material, and 62.64 HRC after the hardening process. On a macroscopic analysis of the samples the unevenness of the hardened layer thickness could be noticed, both in section and along the bearing ring. The measured thickness varied between 7.2 and 11.4 mm. The thickness measurements were performed in the points shown in Figure 2.

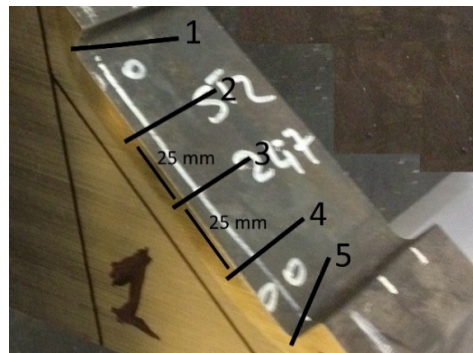


Fig. 2. Surface penetration depth measurement points

The metallographic analysis revealed the type of structure on the hardened area, as well as on the intermediary/interface area and on the raw material. Furthermore, some defects were emphasized after the chemical etch, meant to highlight the structural evolution. These can be observed in Figure 3. The structure of the material, before and after quenching is composed of the following phases: raw material - pearlite, sorbite and $(\text{Fe,Cr})_3\text{C}$ - type carbides; interface material - sorbite, troostite, residual austenite and $(\text{Fe,Cr})_3\text{C}$ - type carbides; quenched material - martensite, residual austenite, and $(\text{Fe,Cr})_3\text{C}$ - type carbides.

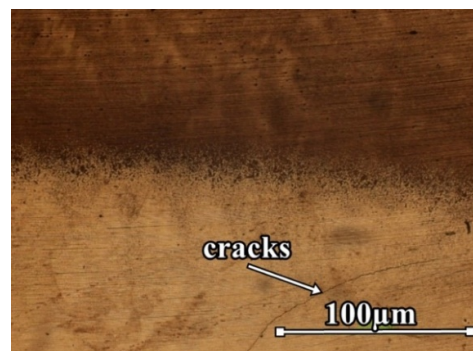


Fig. 3. Cracks in the quenched material

The structure before and after quenching was confirmed by nanoindentation. Nanoindentation measurements were performed using a NHT² nanoindenter from CSM Instruments (Anton Paar), equipped with a Berkovich diamond indenter. The nanoindentation protocol was the following: 50 mN maximum load, 10 second dwell time (in order to minimize the creep effect), loading and unloading rates of 100 mN/min, Oliver & Pharr method of analysis. The result of interest was the instrumented indentation hardness H_{it} . Several matrices of indentations were performed, on slightly etched samples, in order to better position the measurements on the quenched, intermediary and non-treated zones. The variation in hardness in the quenched zone is relatively limited, as can be seen on the surface mapping presented in Figure 4a. Once the intermediary zone and the non-treated zone are reached, the hardness drops gradually, as can be observed in Figure 4b (surface mapping), and 5 (hardness variation as function of distance, starting from the quenched zone ($H_{it} \approx 6500$ MPa), towards the non-treated zone ($H_{it} \approx 3500$ MPa)).

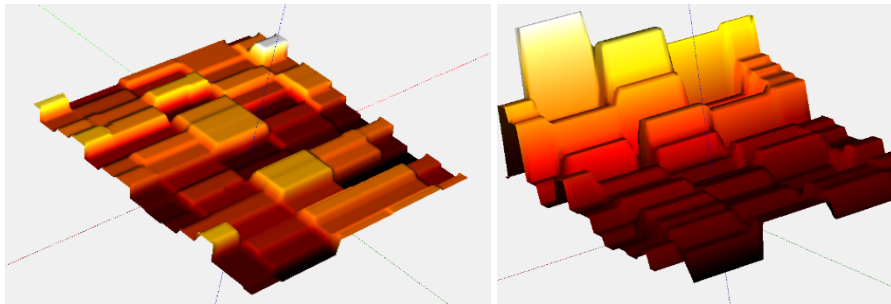


Fig. 4. Hardness mapping of the quenched (a/left), transition and non-treated zones (b/right). Darker regions signify higher hardness

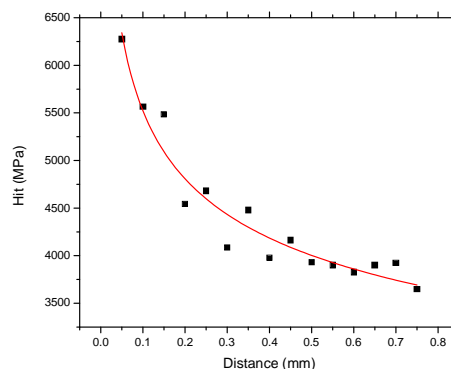


Fig. 5. Hardness variation from the quenched zone, towards the non-treated material

The influence of the process parameters on the uniformity of the thickness of the hardened layer was further studied by means of standard samples manufactured from 50CrMo4 steel. To heat the standard samples, followed by cooling in the quenching medium, an induction coil was used. The schematic and photo of the standard sample placement, inside the inductor, can be observed in Figure 6. The uniformity of the quenched layer as function of power, on the small diameter region of the sample, for

identical periods of heating, was the main focus. Considering the percentage of carbon for this particular grade of steel, the samples were heated up to 870-900 °C, followed by rapid cooling in a polymer based quenching medium. The process factors that have been considered are: i) the distance between the board and the limit of the inductor (this can be changed by moving the sample in the vertical direction); ii) the distance between the rolling path and the inductor (this can be modified by reducing the small diameter of the standard sample (machining) or by eccentric positioning in reference to the inductor).

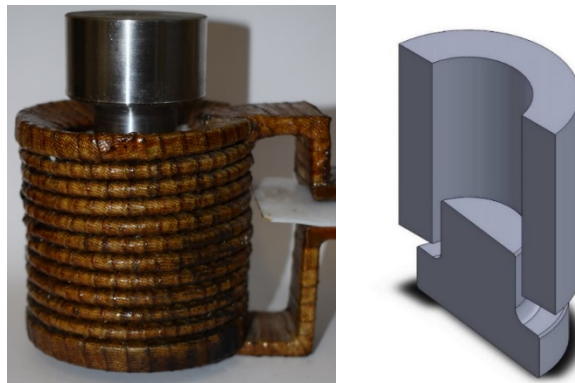


Fig. 6. *Sample placement inside the inductor coil*

Following the thermal treatment stage, the samples were cut lengthwise. The hardness of the material was measured on the width of the samples starting from the edge (the region closest to the inductor), towards the center (the region farthest from the inductor), as well as on the height, starting from the bottom towards the top of the cylinder. The tridimensional variation in hardness can be observed in Figure 7. The results from Figure 7a are obtained on a sample which was heated with 24.2 kW, while the results from Figure 7b are obtained on a sample which was heated with 24.5 kW. One can notice, that for a relatively small increase in power, the penetration depth (hardened layer) is slightly larger (Figure 7b). However, for the sample heated with 24.5 kW, a noticeable drop in hardness, towards the center of the sample, was observed, signifying a non-uniform heating.

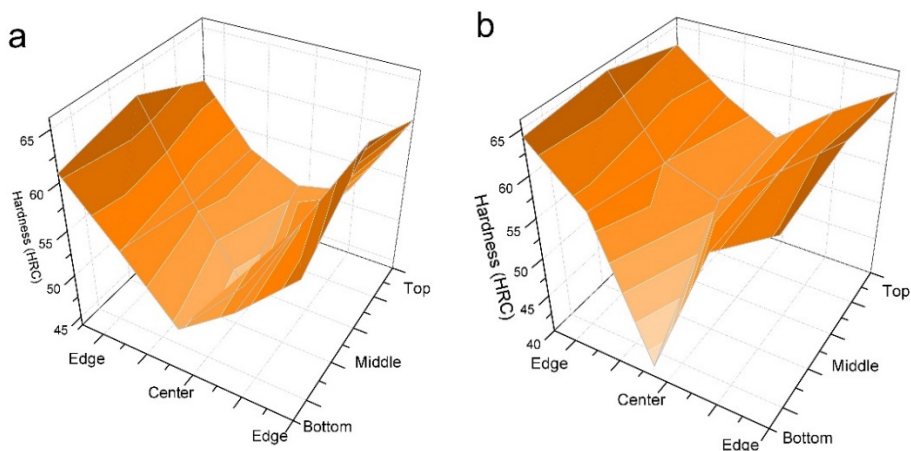


Fig. 7. *Hardness variation as function of the analyzed region*

4. Conclusions

Induction quenching, applied to large diameter bearing rings, can exhibit an uneven depth of the hardened layer in different zones along the ring circumference, uneven depth of the hardened layer in the ring section, and cracks in the bearing material. The influence of the induction heating process parameters was studied. The induction power supplied to the induction coil influences the surface hardening depth on the rolling path, as well as the evenness of the heating towards the center of the material.

Acknowledgments

The authors are acknowledging the funds provided through the PN-III-P2-2.1-BG-2016-0241 project, financed by the Executive Agency for Higher Education, Research, Development and Innovation Funding, and the Romanian Government.

References

1. Chovan, J., Slodička, M.: *Induction Hardening of Steel with Restrained Joule Heating and Nonlinear Law for Magnetic Induction Field: Solvability*. In: Journal of Computational and Applied Mathematics **311** (2017), p. 630-644.
2. Davies, E.J.: *Conduction and Induction Heating*. London. P. Peregrinus Ltd., 1990.
3. Hömberg, D.: *A Numerical Simulation of the Jominy End-Quench Test*. In: Acta Materialia **44** (1996), p. 4375-4385.
4. Hömberg, D.: *A Mathematical Model for the Phase Transitions in Eutectoid Carbon Steel*. In: IMA Journal of Applied Mathematics **54** (1995), p. 31-57.
5. Hömberg, D.: *Irreversible Phase Transitions in Steel*. In: Mathematical Methods in Applied Sciences **20** (1997), p. 59-77.
6. Leblond, J.-B., Devaux, J.: *A New Kinetic Model for Anisothermal Metallurgical Transformations in Steels Including Effect of Austenite Grain Size*. In: Acta Metallurgica **32** (1984), p. 137-146.
7. Montalvo-Urquizo, Liu, J.Q., Schmidt, A.: *Simulation of Quenching Involved In Induction Hardening Including Mechanical Effects*. In: Computational Materials Science **79** (2013), p. 639-649.
8. Şimşir, C., Gur, C.H.: *A FEM Based Framework for Simulation of Thermal Treatments: Application to Steel Quenching*. In: Computational Materials Science **44** (2) (2008), p. 588-600.
9. Verdi, C., Visintin, A.: *A Mathematical Model of the Austenite-Pearlite Transformation in Plain Steel Based On the Scheil's Additivity Rule*. In: Acta Metallurgica **35** (11) (1987), p. 2711-2717.
10. Visintin, A.: *Surface Tension Effects in Phase Transitions*. In: IMA Journal of Applied Mathematics **39** (1987), p. 143-157.
11. Wolff, M., Böhm, M., Böttcher, S.: *Phase Transformations in Steel in the Multi-Phase Case - General Modelling and Parameter Identification*. In: Technical Report 07-02, Universität Bremen, Berichte aus der Technomathematik, 2007.